Running title: **Synergic and antagonist effects of P and Na+ on *Arundo donax***

Impact of high phosphorous and sodium on productivity and stress tolerance of *Arundo donax* plants

Cocozza Claudia[1,*], Brilli Federico[1,*], Miozzi Laura[2], Pignattelli Sara[1], Rotunno Silvia[3], Brunetti Cecilia[4], Giordano Cristiana[4], Pollastri Susanna[1], Centritto Mauro[4], Accotto Gian Paolo[2], Tognetti Roberto[6,7], Loreto Francesco[8]

[1] National Research Council of Italy, Institute for the Sustainable Plant Protection (CNR - IPSP), Via Madonna del Piano 10, 50019 Sesto Fiorentino, Italy

[2] National Research Council of Italy, Institute for the Sustainable Plant Protection (CNR - IPSP), Strada delle Cacce 73, 10135 Torino, Italy

[3] Department of Biosciences and Territory, University of Molise, contrada Fonte Lappone, 86090 Pesche, Italy

[4] National Research Council of Italy, Trees and Timber Institute (CNR - IVALSA), Via Madonna del Piano 10, 50019 Sesto Fiorentino, Italy,

[5] National Research Council of Italy, Institute for Biosciences and Bioresources (CNR - IBBR), Via Madonna del Piano 10, 50019 Sesto Fiorentino, Italy

[6] Department of Agriculture, Environment and Food Sciences, University of Molise, Via Francesco De Sanctis, 86100 Campobasso, Italy

[7] The EFI Project Centre on Mountain Forests (MOUNTFOR), Edmund Mach Foundation, 38010 San Michele all'Adige, Italy

[8] National Research Council of Italy, Department of Biology, Agriculture, and Food Sciences, Piazzale Aldo Moro 7, Roma, Italy

* authors contributed equally to this work

Corresponding author: claudia.cocozza@ipsp.cnr.it; +393332528829

Highlights

Arundo donax is sensitive to elevated salinity. High phosphorous supply to salt-stressed *A. donax* enhances transcriptomic changes that induce the onset of physiological mechanisms of stress tolerance but limits productivity.

Keywords: abiotic stress, giant reed, isoprene emission, phosphorous, salinity, transcriptome

Abstract

Arundo donax L. is an invasive species recently employed for biomass production that emits large amounts of isoprene, a volatile compound having important defensive role. Here, the potential of *A. donax* to grow in degraded soils, characterized by poor fertility, eutrophication and/or salinization, has been evaluated at morphological, biochemical and transcriptional level. Our results highlight sensitivity of *A. donax* to P deficiency. Moreover, we show that *A. donax* response to salt stress (high sodium, Na^+), which impaired plant performance causing detrimental effects on leaf cells ultrastructure, is characterized by enhanced biosynthesis of antioxidant carotenoids and sucrose. Differently from Na^+, high phosphorous (P) supply did not hamper photosynthesis although it affected carbon metabolism through reduction of starch content and by lowering isoprene emission. In particular, we revealed on salt-stress leaves that high P enhanced the expression of genes involved in abiotic stress tolerance, but further increased diffusive limitations to photosynthesis and slowed-down sugar turnover without modifying isoprene emission. Therefore, despite limiting productivity, high P improved *A. donax* tolerance to salinity by favouring the accumulation of carbohydrates that protect cells and increase osmotic potential, and by stimulating the synthesis of antioxidants that improves photo-protection and avoids excessive accumulation of reactive oxygen species.

Introduction

Phosphorus (P) is an essential element for many key enzymes and intermediates of plants photosynthetic CO_2 assimilation and sugar biosynthesis (Beck and Ziegler, 1989). Phosphorous regulates energy storage reactions and maintains structural integrity of cellular membranes (Marschner, 1995). Phosphorous concentration is tightly regulated within the cells because changes in its availability can seriously impair plant physiological processes and structure (Shen *et al.,* 2011). On one hand, P deficiency affects the overall plant metabolism (Hernández *et al.,* 2007) reducing growth (Chiera *et al.,* 2002) and hampering the ability to reproduce and adapt to different environments (Wassen *et al.,* 2005). On the other hand, P surplus decreases plant performances by inhibiting the biosynthesis of starch (Fredeen *et al.,* 1989) and other secondary metabolites (e.g. isoprenoids, Fernández-Martínez *et al.,* 2017, Fares *et al*., 2008), and lowers nitrate assimilation in the roots (Rufty *et al.,* 1990).

Intensive exploitation of phosphate rock reserves for fertilization purposes may lead to their depletion by the end of this century (Cordell *et al.,* 2009). However, marginal lands, where high amounts of P are associated with salinity, are not suitable for agriculture. It is well-know that salinity impairs plant performance and productivity (Munns and Tester, 2008). In particular, exposure to high sodium (Na^+) concentration in soil increases diffusive (Centritto *et al.,* 2003) and biochemical limitations to photosynthetic CO_2 assimilation (Chaves *et al.,* 2009), decreases water transpiration rates, modifies the biosynthesis of both soluble sugars (Dubey and Singh, 1999) and starch (Parida *et al.,* 2002), and reduces pigments content in leaves (Kalaji *et al.,* 2011). Moreover, excess of Na^+ impairs root nutrient uptake by altering the trans-membrane transport of ions that leads to loss of turgor of plant cells and to further membrane damage following the formation of reactive oxygen species (ROS) (Sobhanian *et al.,* 2011).

Arundo donax L., the giant reed, is a non-food perennial rhizomatous invasive grass species belonging to *Poaceae* family (Pilu *et al.,* 2012). *A. donax* is one of the most efficient C3 plant species, able to colonize a wide spectrum of habitats worldwide, from very wet loam to relatively dry sandy soils (Webster *et al.,* 2016). *A. donax* displays a high photosynthetic rate and a fast-growing habit that make its cultivation suitable for biomass and bioenergy production (Webster *et al.,* 2016; Sánchez *et al.,* 2016). In addition, the tolerance to abiotic stress of *A. donax* has been already demonstrated across a range of stressful conditions, thus allowing the exploitation of degraded and marginal lands with *A. donax* crops (Calheiros *et al.,* 2012; Nackley and Kim, 2015). In fact, *A. donax* is able to maintain a high leaf-level photosynthesis and biomass gain under drought (Haworth *et al.,* 2017b) and salinity (Nackley and Kim, 2015). In particular, efficient stomata regulation in *A. donax* is induced by increase in leaf ABA content in response to drought (Haworth *et al.,* 2018). Moreover, *A. donax* is able to adjust the xylem vessel size to regulate the vulnerability to embolism under water deficit conditions (Haworth *et al.,* 2017c). Recently, it has been shown that symbiosis with arbuscular mycorrhiza increases *A. donax* performance to salinity, through proline accumulation and isoprene formation (Pollastri *et al.,* 2018).

A. donax leaves constitutively produce a large amount of isoprene (Velikova *et al.,* 2016), which is known to be involved in mechanisms of protection against abiotic (Vickers *et al.,* 2009) and biotic stresses (Loivamäki *et al.,* 2008). However, there is no clear pattern in isoprene emission in response to abiotic stress in reeds, as isoprene emission increased in *A. donax* following drought (Haworth *et al.,* 2017a), decreased in *Phragmites australis* (the common reed, and a close relative of Arundo) plants exposed to high P concentrations (Fares *et al.,* 2006), and was unaltered in salt-stressed *A. donax* (Pollastri *et al.,* 2018).

In this study, *A. donax* plants grew under controlled laboratory conditions by providing a nutrient solution deprived of P, or enriched with a high concentration of P also in combination with high concentrations of sodium chloride (NaCl). Our investigation aimed at: a) characterizing the response of *A. donax* plants to P availability, both under P-deficiency and supply of high P concentration; b) testing the performance of *A. donax* under multiple (abiotic) stresses, such as a simultaneous excess of P and Na^+. To this purpose, we used an integrated approach, combining physiological and biochemical measurements with transcriptomic analysis. Leaf and root transcriptomes of *A. donax* have been recently explored only in healthy plants (Sablok *et al.,* 2014) and in plants exposed to drought stress (Fu *et al.,* 2016; Evangelistella *et al.,* 2017). Understanding, at molecular level, the response of *A. donax* to combined P and Na^+ stress is crucial for implementing adaptation strategies in order to achieve high biomass yield and productivity in marginal areas for agriculture.

Materials and methods

Plant material, growth conditions, supply of P and Na^+

A. donax plants were propagated from rhizomes of plants collected in Sesto Fiorentino (Italy). Rhizomes were kept in tap water for one day (d) and then planted in 6 dm^3 pots containing quartz sand. All potted plants were then grown in a climatic chamber under controlled environmental conditions (temperature ranging between 24°C and 26°C; relative air humidity ranging between 40% and 60%; photosynthetic photon flux density (PPFD) of 700 µmol m^{-2} s^{-1} for 14 h per d), and were regularly watered twice a week with half strength Hoagland solution (Hoagland and Arnon, 1950) for two months before beginning the experiment.

130 The experiment was performed by applying five different nutrient conditions: 1) Hoagland
131 solution (C); 2) Hoagland solution deprived of phosphorous (-P); Hoagland solution
132 complemented with 8.0 mM KH_2PO_4 (+P); Hoagland solution complemented with 200 mM
133 NaCl (+Na); and Hoagland solution complemented with both 200 mM NaCl and 8.0 mM
134 KH_2PO_4 (+NaP). All different solutions were supplied twice a week during the whole
135 duration of the experiment (43 days).
136
137 **Biometrical traits, leaf determination of C, N, P and Na^+**
138 Biometrical traits (leaf number and culm length) were measured weekly. The relative water
139 content (RWC) of leaves was determined on the second fully expanded leaf at the end of
140 the treatment. Fresh weight (FW) was immediately determined following leaf collection.
141 The same leaf was then immersed into water for 24 h before measuring the turgid weight
142 (TW). Finally, the leaf was oven dried at 80°C for 48 h before measuring the dry weight
143 (DW). RWC was calculated by using the formula:
144 RWC = (FW – DW) / (TW – DW).
145 Total C and total N concentrations (%) were quantified at the end of the treatment with a
146 Carlo Erba NA 1500 CNS Analyzer (Milan, Italy) through the chromatographic column by a
147 thermal conductivity detector.
148 Na^+ and P concentrations were determined at the end of the treatment. Na^+ concentration
149 was measured by flame atomic absorption spectrometry (Analyst 200, Perkin Elmer), and
150 P concentration was measured by inductively coupled plasma atomic emission
151 spectrometry (ICP-AES; iCAP 6500 Duo; ThermoFisher, Dreieich, Germany), employing
152 appropriate quality standard controls (Sreenivasulu *et al.,* 2017).
153
154 **CO_2/H_2O gas exchange, fluorescence and isoprene measurements**

Gas exchange of CO_2 and H_2O and fluorescence measurements were performed at the end of the treatment by using a portable gas exchange system equipped with a fluorometer (Li-Cor 6400, Li-Cor Biosciences Inc., NE, USA). The third (from the shoot apex) fully expanded leaf of *A. donax* was clamped in the 2 cm^2 Li-Cor cuvette and exposed to a saturating PPFD of 1000 µmol m^{-2} s^{-1}, CO_2 concentration of 400 ppm, temperature of 30°C and relative humidity (RH) ranging between 45 and 50%. Photosynthesis (A), stomatal conductance (g_s) and internal CO_2 concentration (Ci) were calculated using the formulations of von Caemmerer and Farqhuar (1981) 10 min after reaching steady-state conditions. The linear electron transport rate (ETR) was calculated from fluorescence measurements of PSII efficiency, according to Genty *et al.* (1989).

Photosynthesis under low O_2 conditions was measured reducing the air O_2 concentration from 21% to 2%. We used a nitrogen cylinder connected with a mass flow controller (Rivoira, Italy) that precisely enriched the concentration of N_2 in the air entering the LI-Cor 6400 from 89 to 99%, while CO_2 concentration was maintained steady at 400 ppm. The O_2 inhibition of photosynthesis was calculated from the A values measured at 21% and at 2% of O_2 (v/v) using the following formula (Zhang *et al.,* 2017):

O_2 inhibition of photosynthesis = (A 2% O_2 – A 21% O_2) * 100/A 2% O_2.

Isoprene emitted by leaves was collected at the end of the treatment after concentrating 3 L of the air exiting from the cuvette in a cartridge filled with 30 mg of Tenax and 30 mg of Carboxen (Gerstel, Mülheim an der Ruhr, Germany). A pump (Elite 5; A.P. Buck, Orlando, FL, USA) set at 200 ml min^{-1} rate was used to fill cartridges with the same volume of air without contamination from air that did not pass through the cuvette. All cartridges were stored at 4°C before being analysed through thermo-desorption followed by gas chromatograph-electro impact mass spectrometry (7890 GC – 5975 MSD 8 Agilent Tech, Santa Clara, CA, USA), as reported in Pollastri *et al.* (2018). Isoprene was identified by

using the NIST 11.L 08 library spectral database and quantified with an isoprene gas standard (99.9%, Sigma-Aldrich) prepared in the laboratory.

During isoprene collection, a charcoal filter (Supelco, Bellafonte, USA) was placed ahead of the Li-Cor 6400 in order to remove all volatile organic compounds (including isoprene) from ambient air before reaching the gas exchange cuvette. Isoprene background was measured every day before starting the measurements by collecting 3 L of air the air exiting the empty cuvette.

RNA sequencing

The first leaf was collected at the end of the treatment for RNA extraction and stored at -80°C. RNA extraction was done with TRIzol® Reagent (Ambion). RNA concentrations and quality were determined with NanoDrop spectrophotometer (Thermo Scientific, Wilmington, USA) and Agilent 2100 Bioanalyzer (Agilent, Santa Clara, CA). According to RNA quality and quantity, three out of four samples for each treatment were chosen for RNA sequencing and sent to the HuGeF sequencing service (http://www.hugef-torino.org, Human Genetics Foundation, Turin, Italy). A total of 15 paired-end libraries (2x75bp) were constructed using the TruSeq RNA library Prep Kit v2 (Illumina, San Diego, CA) with poly-A enrichment and sequenced on Illumina NextSeq 500. Raw data have been deposited in the Sequence Read Archive (https://www.ncbi.nlm.nih.gov/sra) with SRA accession SRP145569. Assessment of read quality metrics was carried out with FastQC software (http://www.bioinformatics.babraham.ac.uk/projects/fastqc/ version 0.11.3). Quality filtering, adapter cutting and trimming were carried out with Trimmomatic (version 0.33) (Bolger *et al.*, 2014), which can handle fastqc paired-end synchronization. After Illumina adapters clipping, the first 12 bases were trimmed due to sequencing biases (Hansen *et al*. 2010), leading and trailing low quality (below 3) or N bases and reads with low average

quality (15) in a 4-bases scan were removed. Finally, reads less than 36 bases long after these steps were dropped.

Trinity software (version 2.0.6) was used for transcripts reconstruction. Contigs less than 200 bp and with coverage less than 5 were discarded (Haas *et al.* 2013). Transcripts redundancy was reduced with CD-HIT software (version 4.6.6), using a word size of 10 and 95% identity (Li and Godzik, 2006). Trinity software was able to assemble a total of 184,849 transcripts (Table S1). After removing redundancy, we obtained a total of 120,553 transcripts. The quality of our reconstructed transcriptome was tested mapping each paired-end library against it; the percentage of reads mapping back to transcriptome (RMBT) were between 78.66% and 89.87%, perfectly concordant with the expected percentage for RNA-seq experiment. In fact, because of the lack of a reference genome, the percentage of multimapping appears greater then single mapping (Table S2). Based on these results, the assembled transcriptome was considered reliable as reference for differential expression analysis.

Identification of differentially expressed genes (DEGs), functional annotation and enrichment analysis

Reads from each of the 15 libraries were mapped against our reference transcriptome and quantified using RSEM (version 1.3.0) (Li and Dewey, 2011). The quantification was obtained as fragment per kb of exon per million fragments mapped (FPKM). In order to identify the differentially expressed genes, Trinity provided scripts based on the R package edgeR (R version 3.3.2; edgeR version 3.16.5) were used. Pairwise comparisons were made to highlight different expression in different conditions. Genes with a false discovery rate cutoff of 0.05 (5% FDR) were considered as differentially expressed.

To annotate the genes, blastx searches were performed against NCBI non-redundant database with an e-value cut-off of $1e^{-3}$. Blastx results, saved as xml files, were loaded into

231 Blast2GO tool (version 4.1; database Germany, DE3, version b2g_jan17) (Conesa and
232 Götz, 2008), and mapping, annotation and InterPro scanning were performed. To
233 associate annotations obtained with Blast2GO to DEGs, the R package Annotation Tools
234 (version 1.44.0) was used (Kuhn *et al.,* 2008). GO enrichment analysis of DEGs was
235 performed on Blast2GO applying Fisher's Exact Test with a FDR of 0.05. Pathways
236 enrichment analysis of DEGs was carried out with KOBAS tool (v3.0) (Xie *et al.,* 2011)
237 using *Oryza sativa* var. *japonica* as reference. Pathways were visualized with KEGG
238 Mapper, a collection of tools for KEGG mapping (Kanehisa *et al.,* 2016).
239
240 **Quantification of metabolites**
241 Soluble carbohydrates were identified and quantified by HPLC-RI analysis at the end of
242 the treatment following the protocol of Tattini *et al.* (1996). Starch was quantified as
243 reported in Chow and Landhäusser (2004) on the pellet resulting from ethanol extraction
244 for the analysis of soluble carbohydrates. Glucose was quantified through peroxidase-
245 glucose oxidase/o-dianisidine reagent (Sigma-Aldrich, Milano, Italy), reading the
246 absorbance at 525 nm after the addition of sulfuric acid.
247 Hydrogen peroxide was measured spectrophotometrically at the end of the treatment after
248 reaction with KI, according to a slightly modified method (Alexieva *et al.,* 2001). A
249 modification of the Sedlak and Lindsay (1968) method was used for the glutathione (GSH)
250 determination at the end of the treatment. Individual carotenoids were identified and
251 quantified at the end of the treatment as reported in García-Plazaola and Becerril (1999).
252 Phenylpropanoids were extracted and purified at the end of the treatment following the
253 protocol of Tattini *et al.* (2004). Abscisic acid (ABA) was extracted and quantified at the
254 end of the treatment using the protocol of López-Carbonell *et al.* (2009).
255

Hydrogen peroxide (H_2O_2) localization and leaf ultrastructure by Transmission Electron Microscopy (TEM)

Hydrogen peroxide localization in leaves was estimated cytochemically via determination of cerium perhydroxyde upon reaction of cerium chloride ($CeCl_3$) with endogenous H_2O_2, following the protocols of Bestwick *et al.* (1997) and Ranieri *et al.* (2003). At the end of the treatment, portion of approximately 0.15 mm^2 were sampled in the center of the leaf blade and then infiltrated (under vacuum) with 5 mM $CeCl_3$ in 50 mM 3-(N-morpholino)-propane sulfonic acid (pH 7.2). The $CeCl_3$-treated and control leaf samples (without $CeCl_3$-staining) were then fixed in 2.5% glutaraldehyde, in 0.2 M phosphate buffer (pH 7.2) for 1 h, and washed twice with the same buffer, prior of post-fixing with 2% osmium tetroxide in phosphate buffer (pH 7.2). Leaves were dehydrated in a graded ethanol series (30, 40, 50, 70, 90 and 100%), and gradually embedded in Spurr Resin (Sigma Aldrich). Ultrathin sections were obtained on an LKB IV ultramicrotome, mounted on Formvar coated copper grids, stained with UranylessEm Stain (Electron Microscopy Science) and lead citrate, and examined by using Philips CM12 transmission electron microscope (Philips, Eindhoven, The Netherlands) operating at 80 kV.

Statistical analyses

Analysis of variance (ANOVA) was applied to test the effect of Na^+ and P supply in *A. donax* plants. LSD post-hoc test was applied to assess significantly different means among treatments ($P < 0.05$ level).

RESULTS

Plant biometrics, gas exchange, chlorophyll fluorescence measurements and isoprene emission

At the end of the experiment, P concentration doubled in +P leaves, but did not decrease significantly in –P leaves, as compared to control (Table 1). In leaves of +Na plants, sodium (Na^+) was two orders of magnitude higher than in control. When Na^+ and P were both provided in excess (+NaP), an increase of Na^+ and a slightly reduced accumulation of P, in comparison to leaves of +Na and +P plants, respectively, was observed.

Excess supply of Na^+ reduced culm length, number of leaves, leaf RWC, and leaf carbon content with respect to control (Table 1). P starvation reduced culm height, leaf number and nitrogen concentration, while P excess did not significantly affect any of the investigated parameters. However, in +NaP plants, culm length, number of leaves, leaf RWC and carbon content decreased to the same extent as in the +Na plants, with respect to control (Table 1).

Photosynthesis of *A. donax* decreased in –P, whereas it was similar to control in +P plants (Table 2). Photosynthesis was inhibited in +Na plants with respect to control, and the effect was even stronger in +NaP plants. In both +Na and +NaP plants, photosynthesis reduction was associated to reduced gs, Ci, and ETR, compared to control (Table 2).

Isoprene emission from *A. donax* leaves was not affected by lack of P but was inhibited in +P plants, in comparison to control (Table 2). Isoprene emission was slight, but non statistically significant, stimulated by the +Na and +NaP treatments. (Table 2).

Analysis of differentially expressed genes (DEGs)

Exposure to high P concentration induced differences in the expression of a higher number of genes in *A. donax* leaves with respect to P starvation (Fig. 1, Table 3). The excess supply of P caused the differential expression of a similar number of up- and down-

303 regulated genes, while the –P treatment mainly induced gene down-regulation. High
304 concentration of Na^+ had a higher impact on the total amount of DEGs (Fig. 1, Table 3),
305 resulting in a higher extent of down-regulated genes with respect to high P treatment (Fig.
306 2). However, the number of DEGs increased 10-fold in +NaP treated plants (Fig. 1, Table
307 3) indicating, at molecular level, a higher response of *A. donax* to the combined (Na^+ and
308 P) than to the singularly applied treatments (Fig. 1, Fig. 2, Table 3). The complete list of
309 DEGs is reported in Table S3.
310 In order to functionally inspect the overall DEGs and identify the major biological
311 processes affected by the different supply of P and Na^+, the transcriptome of *A. donax*
312 leaves was annotated by mean of Gene Ontology (GO). More than half of the transcripts
313 were annotated to at least one GO term (Fig. S1) and the first ten top-hit species found
314 through the blastx search belonged to the *Poaceae* family (Fig. S2), indicating the
315 reliability of the obtained GO annotation.
316 As a result of the GO category enrichment analysis (considering a p-value threshold of
317 0.05), only one functional category ('*catalytic activities*') was significantly over-represented
318 in –P. Whereas, the over-represented categories were 33 (especially '*metabolic*
319 *processes*' and '*localization and transport*') in +P, 38 (especially '*metabolic and*
320 *biosynthetic processes*' involving *'protein binding'*, '*translocation and transportation'*, as
321 well as '*catalytic activities'* and '*biological processes of the extracellular region'*) in +Na,
322 and 139 (especially '*cellular, metabolic and biosynthetic processes of macromolecules and*
323 *organic compounds*' and '*binding activities*', also involving the '*development of anatomical*
324 *structure*' and the '*organization of cellular (and intercellular) parts and organelles'*, as well
325 as '*changes in the extracellular region*') in +NaP plants. A complete overview of all the
326 over-represented functional categories is shown in Table S4.
327

328 **Quantification of soluble carbohydrates and starch, photosynthetic pigments,**
329 **abscisic acid (ABA), hydrogen peroxide (H_2O_2), glutathione (GSH) and caffeic acid**
330 **derivative**

331 Carbohydrate biosynthesis was impaired by different supply of P. However, a reduction of
332 starch content was found in +P leaves, while in –P leaves the content of sucrose, fructose
333 and non-structural carbohydrates was reduced compared to control (Table 4). DEG
334 analysis showed that genes coding for ADP-glucose pyrophosphorylase, soluble acid
335 invertases and a sucrose-phosphate synthase, involved in starch and sucrose metabolism
336 pathway, were down-regulated in both treatments (Table S5). On the opposite, in +Na
337 leaves the content of sucrose doubled compared to control, and +NaP treatment further
338 increased the sucrose content and enhanced two-fold the contents of glucose, fructose,
339 non-structural carbohydrates and starch, compared to control (Table 4). Moreover,
340 pathway analysis on +NaP plants revealed an up-regulation of genes coding for enzymes
341 involved in fructose and glucose synthesis (Table S5, Fig. S3B).

342 In +Na and +NaP leaves, leaf ABA content increased two-fold with respect to control (Fig.
343 3C). In these same leaves, molecular analysis showed a down-regulation of the gene
344 coding for the ABA 8-hydroxylase 3, a key enzyme in ABA catabolism (Table S3).
345 However, three ABA stress-ripening coding genes, involved in response to abiotic stress,
346 were induced in +NaP plants (Table S3).

347 Hydrogen peroxide (H_2O_2) and glutathione (GSH) highly accumulated in +NaP plants with
348 respect to all the other treatments (Fig. 3A, B). Consistent with these observations, genes
349 involved in the glutathione metabolism were more up-regulated in +NaP leaves than in +P
350 leaves (Fig. S3E, Fig. S3F).

351 The content of flavonoids was significantly enhanced in +NaP leaves, while the other
352 treatments caused only a moderate increase of these secondary metabolites, with respect
353 to control (Fig. 3). The pathway of flavonoids biosynthesis was significantly perturbed in

354 +NaP plants. Indeed, genes like flavonol synthase, trans-cinnamate 4-monooxygenase,
355 flavonoid 3'-monooxygenase and chalcone synthase were up-regulated in +NaP plants
356 with respect to control (Fig. S3C, Fig. S3D).
357 Zeaxanthin and β-carotene were enhanced in +Na leaves with respect to control, whereas
358 zeaxanthin and acid caffeic derivatives were further stimulated in +NaP plants (Fig. 3C, D,
359 E, F). Although there was no differential regulation in genes involved in zeaxanthin and β-
360 carotene synthesis in +Na leaves, a down-regulation of lycopene β-cyclase and phytoene
361 synthase, genes responsible for β-carotene synthesis was measured in +NaP plants
362 (Table S3).
363
364 **Transmission electron microscopy images of leaves ultrastructure**
365 The ultrastructure of *A. donax* control leaves highlighted a peripheral location of
366 organelles, and a large vacuole in the center of the cells (Fig. 4). Cytoplasmic organelles
367 (nucleus, mitochondria, vacuole, endoplasmic reticula, Golgi apparatus) showed typical
368 structure and distribution, and chloroplasts had distinct granal and stromal thylakoid
369 arrangement and a well-defined stroma matrix where few and little starch grains were
370 present (Fig. 4B).
371 In +P plants, chloroplasts displayed very little or no starch grains (Fig. 4C), confirming the
372 decrease of starch also reported in Table 3. These cells showed more and bigger
373 plastoglobules than those of control plants (Fig. 4C). In addition, the envelope membrane
374 of few +P chloroplasts appeared damaged, with thylakoids not clearly recognizable (Fig.
375 4C). Some +P cells also had wavy plasma membrane, large peroxisomes (Fig. 4D), and
376 electron dense cerium perhydroxide precipitates in the cell walls after treatment with
377 $CeCl_3$, thus indicating the onset of ROS accumulation and stressful conditions (Fig. 4C;
378 4D).

Chloroplasts of –P leaves were characterized by an extensive system of grana and stroma lamellae (also reported by Hall et al., 1972), filling the stroma, that also contained a moderate number of plastoglobules (Fig. 4E). The nucleus of –P cells showed poorly condensed chromatin. Moreover, deposition of $CeCl_3$ was found in cell walls (Fig. 4F) and in bundle sheath cells.

In leaves of +Na plants, the shape of the cells changed from elliptical to wrinkle elongated, and cell walls appeared curled (indicated by arrows in Fig. 5A). Strong local H_2O_2 accumulation in the cell walls (indicated by the black arrow in Fig. 5B) and large cytoplasmic lipid bodies (Fig. 5B) were detectable in some +Na cells. Moreover, some mesophyll cells were destroyed, and cytoplasmic organelles were no longer recognizable except for swollen or disintegrated chloroplast (Fig. 5C). However, chloroplasts of +Na cells that were still visible showed a wavy outline (indicated by the white arrow in Fig. 5B), significant loss of clear stromal matrix, with swelling and curling thylakoids, and an increased number of plastoglobules (Fig. 5A, 5B). In addition, many peroxisomes with scarce electron dense deposits of $CeCl_3$ were observed (data not shown).

Mesophyll cells of +NaP plants contained chloroplasts with numerous and large plastoglobules and very large starch granules (Fig. 5D), matching the reported increase of starch (Table 3) and carotenoid (i.e., zeaxanthin) content of these leaves (Fig. 2E). Large lipid bodies were also present in the cytoplasm of these cells, and $CeCl_3$ deposits were observed in chloroplasts, peroxisomes and mitochondria (Figs. 5E; 5F).

Discussion

Performance of *Arundo donax* grown under high- or low- concentration of phosphorus (P)

A two-fold increase of P in the leaves of *A. donax* approached toxic levels, as confirmed by early symptoms of alteration of cell ultrastructure and the presence of peroxisomes (Fig. 4D), indicating starting oxidation processes. However, high P concentrations did not hamper *A. donax* growth and photosynthesis (Table 1). Tolerance of photosynthesis to high P concentration could be the result of the tight regulation of P homeostasis within the cytoplasm, due to the activation of mechanisms that transport and store the excess of P into the vacuoles (Mimura *et al.,* 1990). However, excess of P strongly decreased starch accumulation in leaves (Table 4), as confirmed by histological observations (Fig. 4C, D). Our transcriptomics results indicate that the inhibition of starch metabolism in *A. donax* exposed to +P was mainly due to the transcriptional repression of the ADP-glucose pyrophosphorylase, rather than by enhanced translocation of triosophosphates, that reduces the availability of these substrates for starch synthesis in the chloroplasts (Pozueta-Romero *et al*., 1991; Heldt *et al*., 1991). Moreover, in +P plants there was a strong induction of few transcripts coding for cytosolic fructose-1,6- bisphosphatase an enzyme that, by catalyzing the first irreversible reaction that turn fructose-1,6-bisphosphate into fructose-6-phosphate and inorganic phosphate (Ladror *et al*., 1990), plays an important regulatory role in carbohydrates biosynthesis and metabolism (Daie, 1993).

Consistently with previous results (Fares *et al*., 2008) and a recent meta-analysis (Fernández-Martínez *et al*., 2017), leaves of +P plants emitted less isoprene than control and –P plants. Although isoprene production is a highly ATP demanding process (Loreto and Sharkey 1990), exposure to high P concentration may prompt a competition between mitochondrial respiration and the methylerythritol 4-phosphate (MEP) pathway, in turn limiting isoprene biosynthesis (Loreto *et al*., 2007). In particular, phosphoenolpyruvate

426 (PEP) is a substrate for both isoprene biosynthesis and mitochondrial respiration.
427 Mitochondrial respiration was likely stimulated in plants grown at high P concentration
428 (Fares *et al*. 2008). Indeed, we observed an increased transcription of genes involved in
429 energy requiring processes of protein production and export (Fig. S3). Therefore, our
430 results seem to indicate that incorporation of P into PEP, principally serving the respiratory
431 metabolism, made it less available for isoprene production.
432 *A. donax* was sensitive to P deficiency. Although 43 days of P starvation did not
433 significantly decrease the leaf P concentration, in -P leaves the expression of numerous
434 genes was down-regulated (Müller *et al*., 2007; Hernández *et al*., 2007) and the
435 ultrastructure of leaf cells was altered. Further results confirmed that, under reduced P
436 availability, *A. donax* reduces photosynthesis, grows shorter, and produces a lower
437 number of leaves (with reduced N content) than plants grown under normal P availability.
438 Sensitivity to low P availability may affect the capacity of *A. donax* to colonize new habitats
439 (Wassen *et al*., 2005), and limits *A. donax* use for biomass production in poorly fertile soils.
440
441 **Different response of *A. donax* to Na^+ stress, and to synergistic action of high Na^+**
442 **and P**
443 Accumulation of Na^+ in leaves affected stomatal conductance by increasing diffusive
444 limitations of photosynthesis (the acquisition of CO_2 to be assimilated), as further
445 confirmed by low values of Ci. This response to high Na^+ concentrations widely occurs
446 across plant species (Delfine *et al*., 1999; Centritto *et al*., 2003). Stomata closure was
447 likely triggered by increased synthesis of ABA upon salinity stress (Wilkinson and Davies,
448 2002; Seiler *et al*., 2011). In leaves of Na^+-stressed *A. donax*, photosynthesis and ETR
449 were strongly reduced, whereas zeaxanthin and β-carotene were largely synthesized. This
450 suggests the onset of coordinated photochemical processes to inhibit the accumulation of
451 reactive oxygen species (ROS). Salinity stress also stimulated the biosynthesis of sucrose

452 in *A. donax* leaves (Table 4), as also confirmed by the significant over-representation of
453 GO categories related to '*carbohydrate metabolic process*' (Table S4). Beside exerting a
454 signaling role (Park *et al*., 2016), sucrose was likely able to balance the drop in osmotic
455 potential as leaf RWC decreases during progressive exposure to salinity stress (Table 1).
456 However, changes observed to the leaf ultrastructure of Na^+-stressed plants, where only
457 some mesophyll cells and chloroplast resulted completely destroyed (Fig. 5), confirmed
458 that *A. donax* is moderately sensitive to high Na^+ concentration in leaves. Indeed, *A. donax*
459 possesses more glycophytic than halophytic features (Nackley and Kim, 2015) and
460 tolerates salinity through mechanisms that may prevent ROS formation despite
461 accumulation of Na^+ in the leaves (Mumm and Tester, 2008).
462 Salinity impaired photosynthesis but increased (although not significantly) isoprene
463 emission from *A. donax* leaves. Isoprene is synthesized from carbon assimilated through
464 photosynthesis (Delwiche and Sharkey, 1993), but its emission may be also sustained by
465 extra-chloroplastic carbon sources when photosynthesis is limited under (abiotic) stress
466 (Brilli *et al.,* 2007; Fortunati *et al*., 2008). Overall, the simultaneous increases in the
467 biosynthesis of isoprene and carotenoids may imply activation of the 2-C-methyl-D-
468 erythritol 4-phosphate (MEP) pathway in +NaP-stressed *A. donax* plants to enhance
469 protection against stressful condition (Loreto *et al*., 2014; Marino *et al*., 2017).
470
471 An additive effect of simultaneous supply of high Na+ and P concentrations was clearly
472 highlighted by a 10-fold increase in the number of both up- and down-regulated genes in
473 leaves of +NaP *A. donax* plants. Some of the most representative transcription factors
474 already identified in *A. donax* under drought (Fu *et al*., 2016) were also regulated under
475 Na^+ and P stress. Among them, NAC was strongly induced in +Na, +P and +NaP, whereas
476 WRKY 50, 53 and 41 were down-regulated only in +NaP plants. NAC and WRKY genes
477 family are known to mediate water- (Hadiarto and Tran, 2011) and Na^+- stress responses,

as well as ABA signaling pathway in plants (Jiang *et al*., 2017). Genes coding for stress-associated proteins (SAPs) are important regulators of multiple abiotic stress tolerance (Giri *et al*., 2013) and found to be induced in water-stressed *A. donax* plants (Evangelistella *et al*., 2017). However, only two SAPs were down-regulated in +Na and +NaP plants. Despite inducing a higher expression of genes involved in abiotic stress tolerance (e.g., NAC, WRKY and SAP genes), high P concentration exacerbated the reduction of photosynthesis in Na^+-stressed *A. donax* plants, as also indicated by the over-representation of many GO categories related to '*cellular metabolic process*' in +NaP plants (Table S4). Photosynthesis could have been limited by altered sugar metabolism, as the amount of non-structural carbohydrates, fructose, glucose and starch increased two-fold in +NaP plants. It is suggested that combined supply of Na^+ and P strongly reduced the turnover of carbohydrates, which may have favored the formation of large starch grains in the chloroplasts (Fig. 5D, E, F). Our results show that increase of starch biosynthesis in +NaP plants was related (as in +P plants) to the induction of the ADP-glucose pyrophosphorylase, whereas translocation of triosephosphates was not significantly affected. However, in +NaP plants photosynthesis was stimulated under low O_2 conditions, indicating that feedback inhibition of photosynthesis, typically induced by carbohydrates accumulation (Sharkey, 1990; Xu *et al*., 2015) did not occur. The accumulation of carbohydrates induced by P supply in Na^+-stressed plants may serve protective purposes, in enhancing osmotic capacity to assimilate water (Lambers *et al*., 2008) as confirmed by the over-representation of GO categories regarding '*organic substance metabolic process*' in +NaP plants (Table S4). Carbohydrate accumulation may also help prevent damage to the cell structures (Yang and Guo, 2017). Indeed, the +NaP treatment induced a SNF1-related protein kinase coding gene (SnRK2), which was also found to be responsive to both ionic and non-ionic osmotic stressful conditions (Fu *et al*., 2016; Virlouvet and Fromm, 2015). Genes coding for dehydrins (DHNs) proteins, which

play cellular protection in abiotic stress tolerance (Gao and Lan, 2016; Verma *et al*., 2017), were also up-regulated in leaves of +NaP plants. Remarkably we also observed that, while Early Responsive to Dehydration (ERD4) were induced as expected in *Poaceae* (see Fu *et al.,* 2016 for similar finding in drought-stress conditions), two ERD6 genes coding for carbohydrate transporters were down-regulated, consistent with carbohydrates accumulation shown in leaves of +NaP plants.

Interaction between high concentrations of Na^+ and P did not significantly affect isoprene emission, which was once again uncoupled from photosynthesis in stressed leaves (Brilli *et al*., 2007; Vickers *et al*., 2009; Marino *et al*., 2017). The small reduction of isoprene emission with respect to +P leaves could be associated to the very large negative effect of the combined treatment (+NaP) on photosynthesis, and to the consequently reduced photosynthetic substrate entering the MEP pathway. Transcriptomics show up-regulation of ABA biosynthesis and down-regulation of β-carotene (both made by MEP) in +NaP compared to +Na leaves. This suggests a rearrangement of the flux of carbon into the MEP pathway towards hormones controlling stomata movement and away from antioxidants such as isoprene and carotenoids. Moreover, competition with starch for PEP could also limit isoprene synthesis in +NaP as well as in +P leaves (see above). However, starch was not a limiting factor in +NaP leaves as it was in +P leaves. The accumulation of carbohydrates in +NaP leaves was also highlighted by the over-expression of GO categories related to '*organic substance metabolic process*' (Table S4), suggesting that a glucose 6-phosphate shunt might have been activated to increase the availability of precursors for the MEP pathway (Sharkey and Weise, 2017), despite the low flux of carbon fixed by photosynthesis.

In +NaP leaves, a significant increase of both H_2O_2 and glutathione (GSH) contents was observed, and further confirmed in our transcriptome analysis by over-representation of GO categories '*cellular metabolic process' and 'organic substance metabolic process*'

530 (Table S4), indicating enhanced ROS formation and activation of the anti-oxidant
531 metabolism. Moreover, enhanced biogenesis of peroxisomes in +NaP leaf cells (Fig. 5E,
532 F), most likely indicates a general increase of oxidative stress conditions (Lopez-Huertas
533 *et al*., 2000). Peroxisomes contain antioxidants enzymes able to metabolize ROS and to
534 enhance tolerance to a wide range of stresses (Nyathi and Baker, 2006). High synthesis of
535 GSH possibly prevents the increase of H_2O_2 to reach toxic level while allowing this
536 compound to exert signaling functions (Mittler, 2002; Baxter *et al*., 2014) that may further
537 enhance stress response (Knight and Knight, 2001). However, this was clearly insufficient
538 to protect photosynthesis in +NaP leaves.
539

540 **Conclusions**

541 We showed that *A. donax* can be cultivated in marginal soils affected by eutrophication
542 (under high P supply), where it can exert positive functions (e.g. for phytoremediation)
543 despite allocating less carbon to defensive secondary metabolites (isoprene). Moreover,
544 our results highlight that *A. donax* is sensitive to P deficiency and to Na^+ excess, and this
545 sensitivity is further enhanced by the combination of high Na^+ and high P. However, the
546 supply of high P concentrations further stimulates, at molecular and biochemical level,
547 responses that favour stress tolerance in salt-stressed *A. donax*. Therefore, although the
548 productivity of *A. donax* may be largely impaired, the plant adapts and survives in
549 unfavourable soils rich in both P and Na^+.
550

551 **Acknowledgements**

552 The study was funded by research project “CROPSTRESS - System performance of non-
553 food crops to drought stress: development of a plant ideotype”, by the SIR2014 program of
554 the Italian Ministry of University and Research (RBSI14VV35), Claudia Cocozza is the
555 scientific leader of the project. We thank for providing the instrumentation needed for

isoprene Dr. Marco Michelozzi, Laboratory for the Analysis and Research in Environmental Chemistry (ARCA), and for Na and P determination Prof. Cristina Gonnelli.

Author contributions

CC and BF designed the research, analyzed the data and wrote the article with contributions of all the authors; PiS, CC, BF performed research; ML, RS, BC, GC, PoS, MM provided technical assistance; CM, AG, TR, LF supervised and complemented the writing.

Funding information

The study was funded by research project “CROPSTRESS - System performance of non-food crops to drought stress: development of a plant ideotype”, by the SIR2014 program of the Italian Ministry of University and Research (RBSI14VV35), CC is the scientific leader of the project.

571 ## References

572 **Alexieva V, Sergiev I, Mapelli S, Karanov E.** 2001. The effect of drought and ultraviolet
573 radiation on growth and stress markers in pea and wheat. Plant, Cell and Environment **24**,
574 1337-1344.

575 **Ballicora MA, Iglesias AA, Preiss J.** 2004. ADP-glucose pyrophosphorylase: a regulatory
576 enzyme for plant starch synthesis. Photosynthesis Research **79**, 1-24.

577 **Baxter A, Mittler R, Suzuki N.** 2014. ROS as key players in plant stress signalling.
578 Journal of Experimental Botany **65**, 1229–1240.

579 **Beck E, Ziegler P.** 1989. Biosynthesis and degradation of starch in higher plants. Annual
580 Review of Plant Physiology and Plant Molecular Biology **40**, 95–118.

581 **Bestwick CS, Brown IR, Bennett MHR, Mansfield JW.** 1997. Localization of hydrogen
582 peroxide accumulation during the hypersensitive reaction of lettuce cells to *Pseudomonas*
583 *syringae* pv *phaseolicola*. Plant Cell **9**, 209-221.

584 **Bolger AM, Lohse M, Usadel B.** 2014. Trimmomatic: A flexible trimmer for Illumina
585 Sequence Data. Bioinformatics **30**, 2114-20.

586 **Beritognolo I, Piazzai M, Benucci S, Kuzminsky E, Sabatti M, Mugnozza GS, Muleo**
587 **R.** 2007. Functional characterisation of three Italian *Populus alba* L. genotypes under
588 salinity stress. Trees **21**, 465–477.

589 **Brilli F, Ciccioli P, Frattoni M, Prestininzi M, Spanedda AF, Loreto F.** 2009.
590 Constitutive and herbivore-induced monoterpenes emitted by *Populus* × *euroamericana*
591 leaves are key volatiles that orient *Chrysomela populi* beetles. Plant, Cell and Environment
592 **32**, 542-552.

593 **Brilli F, Barta C, Fortunati A, Lerdau M, Loreto F, Centritto M.** 2007. Response of
594 isoprene emission and carbon metabolism to drought in white poplar (*Populus alba*)
595 saplings. New Phytologist **175**, 244-254.

596 **Calheiros CSC, Quiterio PVB, Silva G, Crispim LFC, Brix H, Moura SC, Castro PML.**
597 2012. Use of constructed wetland systems with *Arundo* and *Sarcocornia* for polishing high
598 salinity tannery wastewater. Journal of Environmental Management **95**, 66–71.
599 **Centritto M, Loreto F, Chartzoulakis K.** 2003. The use of low [CO_2] to estimate
600 diffusional and non-diffusional limitations of photosynthetic capacity of salt-stressed olive
601 saplings. Plant, Cell and Environment **26**, 585-594.
602 **Chaves MM, Flexas J, Pinheiro C.** 2009. Photosynthesis under drought and salt stress:
603 regulation mechanisms from whole plant to cell. Annals of Botany **103**, 551–560.
604 **Chow PS, Landhäusser SM.** 2004. A method for routine measurements of total sugar
605 and starch content in woody plant tissues. Tree Physiology **24**, 1129-36.
606 **Conesa A, Götz S.** 2008. Blast2GO: A Comprehensive Suite for Functional Analysis in
607 Plant Genomics. International Journal of Plant Genomics doi:10.1155/2008/619832.
608 **Daie J.** 1993. Cytosolic fructose-1,6-bisphosphatase: a key enzyme in the sucrose
609 biosynthetic pathway. Photosynthesis Research **38**, 5–14.
610 **Ladror US, Latshaw SP, Marcus F.** 1990. Spinach cytosolic fructose1, 6-bisphosphatase.
611 Purification, enzyme properties, and structural comparisons. European Journal of
612 Biochemistry **189**, 89–94.
613 **Delfine S, Alvino A, Villani MC, Loreto F.** 1999. Restrictions to CO_2 conductance and
614 photosynthesis in spinach leaves recovering from salt stress. Plant Physiology **119**, 1101–
615 1106.
616 **Delwiche C, Sharkey T.** 1993. Rapid appearance of ^{13}C in biogenic isoprene when $^{13}CO_2$
617 is fed to intact leaves. Plant, Cell and Environment **16**, 587–591.
618 **Dubey RS, Singh AK.** 1999. Salinity induces accumulation of soluble sugars and alters
619 the activity of sugar metabolising enzymes in rice plants. Biologia Plantarum **42**, 233-239.
620 **Evangelistella C, Valentini A, Ludovisi R, Firrincieli A, Fabbrini F, Scalabrin S,**
621 **Cattonaro F, Morgante M, Scarascia Mugnozza G, Keurentjes JJB, Harfouche A.**

2017. De novo assembly, functional annotation, and analysis of the giant reed (*Arundo donax* L.) leaf transcriptome provide tools for the development of a biofuel feedstock. Biotechnology Biofuels **10**, 138.

Fares S, Barta C, Brilli F, Centritto M, Ederli L, Ferranti F, Pasqualini S, Reale L, Tricoli D, Loreto F. 2006. Impact of high ozone on isoprene emission, photosynthesis and histology of developing *Populus alba* leaves directly or indirectly exposed to the pollutant. Physiologia Plantarum **128**, 456-465.

Fares S, Brilli F, Noguès I, Velikova V, Tsonev T, Dagli S, Loreto F. 2008. Isoprene emission and primary metabolism in *Phragmites australis* grown under different phosphorus levels. Plant Biology **10**, 38-43.

Fernández-Martínez M, Llusià J, Filella I, Niinemets Ü, Arneth A, Wright IJ, Loreto F, Peñuelas J. 2017. Nutrient-rich plants emit a less intense blend of volatile isoprenoids. New Phytology doi.org/10.1111/nph.14889.

Fernando AL, Barbosa B, Costa J, Papazoglou EG. 2016. Chapter 4 - Giant Reed (*Arundo donax* L.): A Multipurpose Crop Bridging Phytoremediation with Sustainable Bioeconomy. Bioremediation and Bioeconomy, Elsevier Inc., 77-95.

Fortunati A, Barta C, Brilli F, Centritto M, Zimmer I, Schnitzler J-P, Loreto F. 2008. Isoprene emission is not temperature-dependent during and after severe drought-stress: A physiological and biochemical analysis. Plant Journal **55**, 687-697.

Fredeen AL, Rao IM, Terry N. 1989. Influence of phosphorus nutrition on growth and carbon partitioning in *Glycine max*. Plant Physiology **89**, 225-230.

Fu Y, Poli M, Sablok G, Wang B, Liang Y, La Porta N, Velikova V, Loreto F, Li M, Varotto C. 2016. Dissection of early transcriptional responses to water stress in *Arundo donax* L. by unigene-based RNA-seq. Biotechnology for Biofuels **9**, 54; DOI 10.1186/s13068-016-0471-8.

Gao J, Lan T. 2016. Functional characterization of the late embryogenesis abundant (LEA) protein gene family from *Pinus tabuliformis* (*Pinaceae*) in *Escherichia coli*. Scientific Reports **6**, 19467.

Gao QM, Venugopal S, Navarre D, Kachroo A. 2011. Low oleic acid-derived repression of jasmonic acid-inducible defense responses requires the WRKY50 and WRKY51 proteins. Plant Physiology **155**, 464-76. doi: 10.1104/pp.110.166876.

García-Plazaola JI, Becerril JM. 1999. A rapid high-performance liquid chromatography method to measure lipophilic antioxidants in stressed plants: simultaneous determination of carotenoids and tocopherols. Phytochemical Analysis **10**, 307–313.

Gechev TS, Hille J. 2005. Hydrogen peroxide as a signal controlling plant programmed cell death. The Journal of Cell Biology **168**, 17–20.

Genty B, Briantis JM, Baker NR. 1989. The relationship between the quantum yield of photosynthetic electron transport and quenching of chlorophyll fluorescence. Biochimica et Biophysica Acta **990**, 87–92.

Giri J, Dansana PK, Kothari KS, Sharma G, Vij S, Tyagi AK. 2013. SAPs as novel regulators of abiotic stress response in plants. BioEssays **35**, 639–48.

Haas BJ, Papanicolaou A, Yassour M, Grabherr M, Blood PD, Bowden J, Couger MB, Eccles D, Li B, Lieber M, Macmanes MD, Ott M, Orvis J, Pochet N, Strozzi F, Weeks N, Westerman R, William T, Dewey CN, Henschel R, Leduc RD, Friedman N, Regev A. 2013. De novo transcript sequence reconstruction from RNA-seq using the Trinity platform for reference generation and analysis. Nature Protocols **8**, 1494-512.

Hadiarto T, Tran LSP. 2011. Progress studies of drought-responsive genes in rice. Plant Cell Reports 30, 297–310.

Hall JD, Barr R, Al-Abbas AH, Crane FL. 1972. The ultrastructure of chloroplasts in mineral-deficient maize leaves. Plant Physiology **50**, 404–409.

672 **Hansen KD, Brenner SE, Dudoit S.** 2010. Biases in Illumina transcriptome sequencing
673 caused by random hexamer priming. Nucleic Acids Research **38**, 131.

674 **Haworth M, Catola S, Marino G, Brunetti C, Michelozzi M, Riggi E, Avola G,**
675 **Cosentino LS, Loreto F, Centritto M.** 2017a. Moderate drought stress induces increased
676 foliar dimethylsulphoniopropionate (DMSP) concentration and isoprene emission in two
677 contrasting ecotypes of *Arundo donax*. Frontiers in Plant Science **8**, 1016; doi:
678 10.3389/fpls.2017.01016.

679 **Haworth M, Cosentino LS, Marino G, Brunetti C, Scordia D, Testa G, Riggi E, Avola**
680 **G, Loreto F, Centritto M.** 2017b. Physiological responses of *Arundo donax* ecotypes to
681 drought: a common garden study. GCB Bioenergy **9**, 132-143.

682 **Haworth M, Centritto M, Giovannelli A, Marino G, Proietti N, Capitani D, De Carlo A,**
683 **Loreto F.** 2017c. Xylem morphology determines the drought response of two *Arundo*
684 *donax* ecotypes from contrasting habitats. GCB Bioenergy **9**, 119–131.

685 **Haworth M, Marino G, Cosentino LS, Brunetti C, De Carlo A, Avola G, Riggi E, Loreto**
686 **F, Centritto M.** 2018. Increased free abscisic acid during drought enhances stomatal
687 sensitivity and modifies stomatal behaviour in fast growing giant reed (*Arundo donax*).
688 Environmental and Experimental Botany **147**, 116-124.

689 **Heldt HW, Flügge U-I, Borchert S.** 1991. Diversity of specificity and function of
690 phosphate translocators in various plastids. Plant Physiology **95,** 341–343.

691 **Hernández G, Ramírez M, Valdés-López O, Tesfaye M, Graham MA, Czechowski T,**
692 **Schlereth A, Wandrey M, Erban A, Cheung F, Wu HC, Lara M, Town CD, Kopka J,**
693 **Udvardi MK, Vance CP.** 2007. Phosphorus stress in common bean: root transcript and
694 metabolic responses. Plant Physiology **144**, 752–767,

695 **Hewitt CN, Monson RK, Fall R.** 1990. Isoprene emissions from the grass *Arundo donax*
696 L. are not linked to photorespiration. Plant Science **66**, 139-144.

Hoagland DR, Arnon DI. 1950. The water-culture method for growing plants without soil. California Agricultural Experiment Station Circural **347**, 1–39.

Hu J, Aguirre M, Peto C, Alonso J, Ecker J, Chory J. 2002. A role for peroxisomes in photomorphogenesis and development of Arabidopsis. Science **297**, 405-9.

Ji T, Li S, Huang M, Di Q, Wang X, Wei M, Shi Q, Li Y, Gong B, Yang F. 2017. Overexpression of cucumber phospholipase D alpha gene (CsPLDα) in tobacco enhanced salinity stress tolerance by regulating Na+–K+ balance and lipid peroxidation. Frontiers in Plant Science **8**, 499.

Jiang J, Ma S, Ye N, Jiang M, Cao J, Zhang J. 2017. WRKY transcription factors in plant responses to stresses. Journal of Integrative Plant Biology **2**, 86-101.

Kalaji H, Govindjee K, BosaKoscielniak J, Zuk-Golaszewska K. 2011. Effects of salt stress on photosystem II efficiency and CO_2 assimilation of two Syrian barley land races. Environmental and Experimental Botany **73**, 64–72.

Kanehisa M, Sato Y, Kawashima M, Furumichi M, Tanabe M. 2016. KEGG as a reference resource for gene and protein annotation. Nucleic Acids Research **44**, D457-D462

Kang J-H, McRoberts J, Shi F, Moreno JE, Jones AD, Howe GA. 2014. The flavonoid biosynthetic enzyme chalcone isomerase modulates terpenoid production in glandular trichomes of tomato. Plant Physiology **164**, 1161–1174.

Kaur N, Reumann S, Hu J. 2009. Peroxisome biogenesis and function. In: Somerville CR, Meyerowitz EM (eds) The Arabidopsis book. The American Society of Plant Biologists, Rockville, MD, USA, pp 1–41.

Kerepesi I, Galiba G. 2000. Osmotic and salt stress-induced alteration in soluble carbohydrate content in wheat seedlings. Crop Science **40**, 482-487.

Knight H, Knight MR. 2001. Abiotic stress signalling pathways: specificity and cross-talk. Trends in Plant Science **6**, 262-267.

723 **Ku MSB, Agarie S, Nomura M, Fukayama H, Tsuchida H, Ono K, Hirose S, Toki S,**
724 **Miyao M, Matsuoka M.** 1999. High level expression of maize phosphoenolpyruvate
725 carboxylase in transgenic rice plants. Nature Biotechnology **17**, 76–80.

726 **Kuhn A, Luthi-Carter R, Delorenzi M.** 2008. Cross-species and cross-platform gene
727 expression studies with the Bioconductor-compliant R package annotation Tools. BMC
728 Bioinformatics **9**, 26.

729 **Laisk A, Loreto F.** 1996. Determining photosynthetic parameters from leaf CO_2 exchange
730 and chlorophyll fluorescence (ribulose-1,5-bisphosphate carboxylase/oxygenase specificity
731 factor, dark respiration in the light, excitation distribution between photosystems,
732 alternative electron transport rate, and mesophyll diffusion resistance). Plant Physiology
733 **110**, 903–912.

734 **Lambers H, Chapin III, Pons FSTL.** 2008. Plant Physiological Ecology. 2nd edition.
735 Springer, New York.

736 **Li B, Dewey CN.** 2011. RSEM: accurate transcript quantification from RNA-Seq data with
737 or without a reference genome. BMC Bioinformatics **12**, 323.

738 **Li W, Godzik A.** 2006. Cd-hit: a fast program for clustering and comparing large sets of
739 protein or nucleotide sequences. Bioinformatics **22**, 1658-1659.

740 **Loivamäki M, Mumm R, Dicke M, Schnitzler JP.** 2008. Isoprene interferes with the
741 attraction of bodyguards by herbaceous plants. Proceedings of the National Academy of
742 Sciences **105**, 17211-2.

743 **López-Carbonell M, Gabasa M, Jáuregui O.** 2009. Enhanced determination of abscisic
744 acid (ABA) and abscisic acid glucose ester (ABA-GE) in *Cistus albidus* plants by liquid
745 chromatography-mass spectrometry in tandem mode. Plant Physiology and Biochemistry
746 **47**, 256-261.

747 **Lopez-Huertas E, Charlton W, Johnson B, Graham I, Baker A.** 2000. Stress induces
748 peroxisome biogenesis genes. EMBO Journal **19**, 6770-6777.

Loreto F, Sharkey TD. 1990. A gas exchange study of photosynthesis and isoprene emission in red oak. Planta **182**, 523-531.

Loreto F, Delfine S. 2000. Emission of isoprene from salt-stressed *Eucalyptus globulus* leaves. Plant Physiology **123**, 1605–1610.

Loreto F, Centritto M, Barta C, Calfapietra C, Fares S, Monson RK. 2007. The relationship between isoprene emission rate and dark respiration rate in white poplar (*Populus alba* L.) leaves. Plant, Cell and Environment **30**, 662-669.

Loreto F, Pollastri S, Fineschi S, Velikova V. 2014. Volatile isoprenoids and their importance for protection against environmental constraints in the Mediterranean area. Environmental and Experimental Botany **103**, 99–106.

Machado RMA, Serralheir RP. 2017. Soil salinity: effect on vegetable crop growth. management practices to prevent and mitigate soil salinization. Horticulturae **3**, 30; doi:10.3390/horticulturae3020030.

Marino G, Brunetti C, Tattini M, Romano A, Biasioli F, Tognetti R, Loreto F, Ferrini F, Centritto M. 2017. Dissecting the role of isoprene and stress-related hormones (ABA and ethylene) in *Populus nigra* exposed to unequal root zone water stress. Tree Physiology **37**, 1637-1647.

Marschner H. 1995. Mineral nutrition of higher plants. Second edition, Functions of Mineral Nutrients: Macronutrient, Academic Press Inc. (Elsevier) **8**, 229–312.

Mimura T, Dietz K, Kaiser W, Schramm M, Kaiser G, Heber U. 1990. Phosphate transport across biomembranes and cytosolic phosphate homeostasis in barley leaves. Planta **180**, 139–146.

Mittler R. 2002. Oxidative stress, antioxidants and stress tolerance. Trends in Plant Science **7**, 405–410.

773 **Müller R, Morant M, Jarmer H, Nilsson L, Nielsen TH.** 2007. Genome-wide analysis of
774 the Arabidopsis leaf transcriptome reveals interaction of phosphate and sugar metabolism.
775 Plant Physiology **143**, 156–171.

776 **Munns R, Tester M.** 2008. Mechanisms of Salinity Tolerance. Annual Review of Plant
777 Biology **9**, 651-681.

778 **Nackley L, Kim SH.** 2015. A salt on the bioenergy and biological invasions debate: salinity
779 tolerance of the invasive biomass feedstock *Arundo donax*. GCB Bioenergy **7**, 752–762.

780 **Nackley LL, Vogt KA, Kim SH.** 2014. *Arundo donax* water use and photosynthetic
781 responses to drought and elevated CO_2. Agricultural, Water and Management **136**, 13–22.

782 **Nordberg GF, Fowler B, Nordberg M** (2007). Handbook on the Toxicology of Metals.
783 Third edition. Salt Lake City, UT: Academic Press.

784 **Owen S, Peñuelas J.** 2005. Opportunistic emissions of volatile isoprenoids. Trends in
785 Plant Science **10** 420-426.

786 **Papazoglou EG.** 2007. *Arundo donax* L. stress tolerance under irrigation with heavy metal
787 aqueous solutions. Desalination **211**, 304–313.

788 **Parida A, Das AB, Das P.** 2002. NaCl stress causes changes in photosynthetic pigments,
789 proteins and other metabolic components in the leaves of a true mangrove, *Bruguier*
790 *aparviflora*, in hydroponic cultures. Journal of Plant Biology **45**, 28-36.

791 **Park HJ, Kim W-Y, Yun D-J.** 2016. A new insight of salt stress signaling in plant.
792 Molecules and Cells **39**, 447-459.

793 **Peñuelas J, Sardans J, Rivas-Ubach A, Janssens IV.** 2012. The human-induced
794 imbalance between C, N and P in Earth's life system. Global Change and Biology **18**, 3–6.

795 **Peñuelas J, Poulter B, Sardans J, Ciais P, van der Velde M, Bopp L, Boucher O,**
796 **Godderis Y, Hinsinger P, Llusia J, Nardin E, Vicca S, Obersteiner M, Janssens IA.**
797 2013. Human-induced nitrogen–phosphorus imbalances alter natural and managed

798 ecosystems across the globe. Nature Communications **4**, 2934, DOI:
799 10.1038/ncomms3934.

800 **Pilu R, Bucci A, Badone FC, Landoni M.** 2012. Giant reed (*Arundo donax* L.): a weed
801 plant or a promising energy crop? African Journal of Biotechnology **11**, 9163–9174.

802 **Pollastri S, Savvides A, Pesando M, Lumini E, Volpe MG, Ozudogru EA, Faccio A, De**
803 **Cunzo F, Michelozzi M, Lambardi M, Fotopoulos V, Loreto F, Centritto M, Balestrini**
804 **R.** 2018. Impact of two arbuscular mycorrhizal fungi on *Arundo donax* L. response to salt
805 stress. Planta **247**, 573–585.

806 **Pompeiano A, Vita F Alpi A, Guglielminetti L.** 2015. *Arundo donax* L. response to low
807 oxygen stress. Environmental and Experimental Botany **111**, 147–154.

808 **Portis AR.** 1992. Regulation of ribulose-1,5-bisphosphate carboxylase/oxygenase activity.
809 Annual Review of Plant Physiology and Plant Molecular Biology **43**, 415-37.

810 **Pozueta-Romero J, Frehner M, Viale AM, Akazawa T.** 1991. Direct transport of ADP
811 glucose by an adenylate translocator is linked to starch biosynthesis in amyloplasts.
812 Proceedings of the National Academy of Sciences **88**, 5769-5773.

813 **Ramel F, Birtic S, Cuiné S, Triantaphylidès C, Ravanat J-L, Havaux M.** 2012. Chemical
814 quenching of singlet oxygen by carotenoids in plants. Plant Physiology **158**, 1267–1278.

815 **Ranieri A, Castagna A, Pacini J, Baldan B, Mensuali Sodi A, Soldatini GF.** 2003. Early
816 production and scavenging of hydrogen peroxide in the apoplast of sunflower plants
817 exposed to ozone. Journal of Experimental Botany **54**, 2529-2540.

818 **Rasmussen R.** 2001. Quantification on the Light Cycler instrument. In: Meuer S, Wittwer
819 C, Nakagawara K, eds. Rapid Cycle Real-Time PCR: Methods and Applications.
820 Heidelberg: Springer-Verlag Press, pp. 21–34.

821 **Rosenstiel TN, Potosnak MJ, Griffin KL, Fall R, Monson RK.** 2003. Increased CO_2
822 uncouples growth from isoprene emission in an agriforest ecosystem. Nature **421**, 256-
823 259.

824 **Rufty TW Jr., MacKown CT, Israel DW.** 1990. Phosphorus stress effects on assimilation
825 of nitrate. Plant Physiology **94**, 328–333.

826 **Sablok G, Fu Y, Bobbio V, Laura M, Rotino GL, Bagnaresi P, Allavena A, Velikova V,**
827 **Viola R, Loreto F, Li M, Varotto C.** 2014. Fuelling genetic and metabolic exploration of
828 C3 bioenergy crops through the first reference transcriptome of *Arundo donax* L. Plant
829 Biotechnology Journal **12**, 554–567.

830 **Sánchez E, Gil S, Azcón-Bieto J, Nogués S.** 2016. The response of *Arundo donax* L.
831 (C3) and *Panicum virgatum* (C4) to different stresses. Biomass and Bioenergy **85**, 335-
832 345.

833 **Sedlak J, Lindsay RH.** 1968. Estimation of total, protein-bound, and nonprotein sulfhydryl
834 groups in tissue with Ellman's reagent. Analytical Biochemistry **25**, 192-205.

835 **Seiler C, Harshavardhan VT, Rajesh K, Reddy PS, Strickert M, Rolletschek H, Scholz**
836 **U, Wobus U, Sreenivasulu N.** 2011. ABA biosynthesis and degradation contributing to
837 ABA homeostasis during barley seed development under control and terminal drought-
838 stress conditions. Journal of Experimental Botany **62**, 2615–2632.

839 **Sharkey TD.** 1990. Feedback limitation of photosynthesis and the physiological role of
840 ribulose bisphosphate carboxylase carbamylation. Botanical Magazine, Tokyo **2**, 87–105.

841 **Sharkey T, Weise SE.** 2017. The glucose 6-phosphate shunt around the Calvin-Benson
842 cycle. Journal of Experimental Botany **68**, 4067–4077.

843 **Sharkey TD, Yeh S.** 2001. Isoprene emission from plants. Annual Review of Plant
844 Physiology and Plant Molecular Biology **52**, 407-436.

845 **Shen J, Yuan L, Zhang J, Li H, Bai Z, Chen X, Zhang W, Zhang F.** 2011. Phosphorus
846 dynamics: from soil to plant. Plant Physiology **156**, 997–1005.

847 **Smith VH, Tilman GD, Nekola JC.** 1999. Eutrophication: impacts of excess nutrient
848 inputs on freshwater, marine, and terrestrial ecosystems. Environmental Pollution **100**,
849 179-196.

Sobhanian H, Aghaei K, Komatsu S. 2011. Changes in the plant proteome resulting from salt stress: toward the creation of salt-tolerant crops? Journal of Proteomics **74**, 1323–1337.

Sreenivasulu V, Kumar NS, Dharmendra V, Asif M, Balaram V, Zhengxu H, Zhen Z. 2017. Determination of boron, phosphorus, and molybdenum content in biosludge samples by microwave plasma atomic emission spectrometry (MP-AES). Applied Science **7**, 264; doi:10.3390/app7030264.

Tattini M, Galardi C, Pinelli P, Massai R, Remorini D, Agati G. 2004. Differential accumulation of flavonoids and hydroxycinnamates in leaves of *Ligustrum vulgare* under excess light and drought stress. New Phytologist **163**, 547–561.

Tattini M, Gucci R, Romani A, Baldi A, Everard JD. 1996. Changes in non-structural carbohydrates in olive (*Olea europaea* L.) leaves during root zone salinity stress. Physiologia Plantarum **98**, 117–124.

Tiessen H. 2011. Phosphorus Availability in the Environment. In: eLS. John Wiley & Sons Ltd, Chichester, doi: 10.1002/9780470015902.a0003188.pub2.

Tilman D, Cassman KG, Matson PA, Naylor R, Polasky S. 2002. Agricultural sustainability and intensive production practices. Nature **418**, 671-677.

Velikova V, Brunetti C, Tattini M, Doneva D, Ahrar M, Tsonev T, Stefanova M, Ganeva T, Gori A, Ferrini F, Varotto C, Loreto F. 2016. Physiological significance of isoprenoids and phenylpropanoids in drought response of *Arundinoideae* species with contrasting habitats and metabolism. Plant, Cell and Environment **39**, 2185-2197.

Verma G, Dhar YV, Srivastava D, Kidwai M, Chauhan PS, Bag SK, Asif MH, Chakrabarty D. 2017. Genome-wide analysis of rice dehydrin gene family: Its evolutionary conservedness and expression pattern in response to PEG induced dehydration stress. PLoS One **12**, e0176399.

875 **Vickers CE, Gershenzon J, Lerdau MT, Loreto F.** 2009. A unified mechanism of action
876 for volatile isoprenoids in plant abiotic stress. Nature Chemical Biology **5**, 283–291.
877 **Virlouvet L, Fromm M.** 2015. Physiological and transcriptional memory in guard cells
878 during repetitive dehydration stress. New Phytologist **205**, 596–607.
879 **von Caemmerer S, Farquhar GD.** 1981. Some relationships between the biochemistry of
880 photosynthesis and the gas exchange of *Phaseolus vulgaris* cultivar Hawkesbury Wonder
881 leaves. Planta **153**, 376–387.
882 **Wassen MJ, Venterink HO, Lapshina ED, Tanneberger F.** 2005. Endangered plants
883 persist under phosphorus limitation. Nature **437**, 547-550.
884 **Webster RJ, Driever SM, Kromdijk J, McGrath J, Leakey ADB, Siebke K,**
885 **Demetriades-Shah T, Bonnage S, Peloe T.** 2016. High C3 photosynthetic capacity and
886 high intrinsic water use efficiency underlies the high productivity of the bioenergy grass
887 *Arundo donax*. Scientific Reports **6**, 20694.
888 **Wilkinson S, Davies WJ.** 2002. ABA-based chemical signalling: the coordination of
889 responses to stress in plants. Plant, Cell and Environment **25**, 195–210.
890 **Wingler A, Lea PJ, Quick WP, Leegood RC.** 2000. Photorespiration: metabolic pathways
891 and their role in stress protection. Philosophical Transactions of the Royal Society B:
892 Biological Sciences **355**, 1517-1529.
893 **Xie C, Mao X, Huang J, Ding Y, Wu J, Dong S, Kong L, Gao G, Li C-H, Wei L.** 2011.
894 KOBAS 2.0: a web server for annotation and identification of enriched pathways and
895 diseases. Nucleic Acids Research **39**, W316–W322.
896 **Xu Z, Jiang Y, Zhou G.** 2015. Response and adaptation of photosynthesis, respiration,
897 and antioxidant systems to elevated CO_2 with environmental stress in plants. Frontiers in
898 Plant Science **6**, 701.
899 **Yang Y, Guo Y.** 2017. Elucidating the molecular mechanisms mediating plant salt-stress
900 responses. New Phytologist **217**, 523–539.

Zeeman SC, Smith SM, Smith AM. 2004. The breakdown of starch in leaves. New Phytologist **163**, 247–261.

Zhang ZS, Liu MJ, Scheibe R, Selinski J, Zhang LT, Yang C, Meng XL, Gao HY. 2017. Contribution of the alternative respiratory pathway to PSII photoprotection in C3 and C4 Plants. Molecular Plant **10**, 131–142.

Table 1. Plant biometrical traits (culm length and leaf number), relative water content (RWC), carbon, nitrogen (N), sodium (Na) and phosphorous (P) contents in leaves of *Arundo donax* plants in control conditions (C), without phosphorous supply (-P), with excess supply of phosphorous (+P) or sodium chloride (+Na), and with excess supply of both phosphorous and sodium chloride (+NaP). Data are means of 4 plants per treatment ± SE; different letters indicate statistical difference at $P < 0.05$ in the same column.

	culm lenght (cm)	leaf number (n)	RWC (%)	carbon (%)	N (%)	Na (µg g^{-1} DW)	P (µg g^{-1} DW)
C	90.8 ± 2.0 ^{a}	16.0 ± 0.2 ^{ab}	89.6 ± 2.1 ^{a}	42.4 ± 0.3 ^{a}	3.4 ± 0.2 ^{a}	120.9 ± 23.1 ^{c}	2358.7 ± 168.4 ^{c}
-P	81.54 ± 2.9 ^{b}	15.2 ± 0.5 ^{b}	90.1 ± 0.6 ^{a}	42.4 ± 0.3 ^{a}	2.9 ± 0.2 ^{b}	103.5 ± 31.8 ^{c}	1766.7 ± 154.4 ^{c}
+P	91.3 ± 4.3 ^{a}	16.8 ± 0.5 ^{a}	91.5 ± 0.6 ^{a}	41.3 ± 0.6 ^{a}	3.7 ± 0.1 ^{a}	151.2 ± 16.3 ^{c}	5765.4 ± 403.2 ^{a}
+Na	62.6 ± 3.6 ^{c}	11.5 ± 0.3 ^{c}	83.0 ± 2.7 ^{b}	40.3 ± 0.5 ^{b}	3.8 ± 0.1 ^{a}	15098.3 ± 1128.1 ^{b}	2100.7 ± 109.0 ^{c}
+NaP	66.4 ± 2.5 ^{c}	10.7 ± 0.3 ^{c}	82.3 ± 1.1 ^{b}	39.5 ± 0.1 ^{b}	3.4 ± 0.1 ^{a}	17781.4 ± 1567.9 ^{a}	4501.3 ± 297.2 ^{b}

Table 2. Photosynthesis (A), O_2 inhibition of photosynthesis (%), stomatal conductance (g_s), internal CO_2 concentrations (Ci) electron transport rate (ETR), isoprene emission of *Arundo donax* plants in control (C) conditions, without phosphorous supply (-P), with excess supply of phosphorous (+P) or sodium chloride (+Na), and with excess supply of both phosphorous and sodium chloride (+NaP). Data are means of 4 plants per treatment ± SE; different letters indicate statistical difference at $P < 0.05$ in the same column.

	A (μmol m^{-2} s^{-1})	Inhibition of photosynthesis (%)	g_s (mol m^{-2} s^{-1})	Ci (ppm)	ETR	Isoprene (nmol m^{-2} s^{-1})
C	23.4 ± 1.1 ^{a}	29.9 ± 3.7 ^{b}	0.32 ± 0.03 ^{a}	239 ± 11 ^{a}	159 ± 5 ^{a}	17.9 ± 2.8 ^{a}
-P	18.2 ± 0.4 ^{b}	18.3 ± 2.8 ^{b}	0.24 ± 0.03 ^{a}	245 ± 16 ^{a}	140 ± 7 ^{a}	20.7 ± 4.4 ^{a}
+P	21.4 ± 1.2 ^{a}	26.2 ± 2.7 ^{b}	0.30 ± 0.05 ^{a}	250 ± 11 ^{a}	149 ± 6 ^{a}	12.0 ± 2.9 ^{b}
+Na	12.5 ± 2.0 ^{c}	48.3 ± 9.5 ^{a}	0.08 ± 0.03 ^{b}	167 ± 14 ^{b}	103 ± 19 ^{b}	25.9 ± 5.4 ^{a}
+NaP	4.0 ± 0.5 ^{d}	49.9 ± 12.2 ^{a}	0.03 ± 0.00 ^{c}	158 ± 21 ^{b}	71 ± 5 ^{b}	20.7 ± 3.3 ^{a}

Table 3.

Number of differentially expressed genes (DEGs) at 5% FDR; (-P) low phosphorous, (+P) excess of phosphorous, (+Na) excess of sodium chloride, (+NaP) excess of both phosphorous and sodium chloride, (C) control condition.

	-P vs C	**+P vs C**	**+Na vs C**	**+NaP vs C**
Up-regulated genes	75	258	243	2103
Down-regulated genes	234	198	453	3076
Total number of DEGs	**309**	**456**	**696**	**5179**

Table 4. Carbohydrates and starch content in leaves of *Arundo donax* plants in control conditions (C), without phosphorous supply (-P), with excess supply of phosphorous (+P) or sodium chloride (+Na), and with an excess supply of both phosphorous and sodium chloride (+NaP). Data are means of 4 plants per treatment ± SE; different letters indicate statistical difference at $P < 0.05$ in the same column.

	sucrose (mg g^{-1} DW)	glucose (mg g^{-1} DW)	fructose (mg g^{-1} DW)	non-structural carbohydrates (mg g^{-1} DW)	starch (mg g^{-1} DW)
C	4.4 ± 0.4 ^{c}	14.9 ± 0.5 ^{b}	67.8 ± 2.9 ^{b}	87.0 ± 3.6 ^{b}	5.2 ± 0.2 ^{b}
-P	3.3 ± 0.2 ^{c}	11.6 ± 0.5 ^{b}	45.1 ± 0.9 ^{c}	60.0 ± 14.5 ^{c}	4.8 ± 0.4 ^{bc}
+P	4.2 ± 0.3 ^{c}	14.2 ± 0.9 ^{b}	73.0 ± 4.6 ^{b}	91.4 ± 4.2 ^{b}	1.8 ± 0.5 ^{c}
+Na	11.4 ± 0.3 ^{b}	15.0 ± 0.8 ^{b}	71.4 ± 1.7 ^{b}	97.8 ± 2.7 ^{b}	4.3 ± 0.3 ^{b}
+NaP	14.1 ± 0.6 ^{a}	37.3 ± 2.7 ^{a}	166.0 ± 10.6 ^{a}	217.4 ± 13.1 ^{a}	7.1 ± 0.2 ^{a}

Figure legends

Figure 1. Venn diagram of differentially expressed genes (FDR<0.05) in *Arundo donax* plants without phosphorous supply (-P), with excess supply of phosphorous (+P) or sodium chloride (+Na), and with an excess supply of both phosphorous and sodium chloride (+NaP) with respect to control condition.

Figure 2. Volcano plots showing the entity of differentially expressed genes (DEGs) in *Arundo donax* plants without phosphorous supply (a: -P), with excess supply of phosphorous (b: +P) or sodium chloride (c: +Na), and with an excess supply of both phosphorous and sodium chloride (d: +NaP) with respect to control conditions. The log_2-fold change (logFC) for each gene is plotted against log_{10}-fold Fold Discovery Rate (logFDR). Significantly DEGs at 5% FDR are highlighted in grey.

Figure 3 – Hydrogen peroxide (H_2O_2) (A), glutathione (GSH) (B), abscisic acid (ABA) (C), caffeic acid derivative (D), zeaxanthin (E) and β-carotene (F) contents of *A. donax* plants in control (C) conditions, without phosphorous supply (-P), with excess supply of phosphorous (+P) or of sodium chloride (+Na), and with an excess supply of both phosphorous and sodium chloride (+NaP). Data are means of 4 plants per treatment ± SE; different letters indicate statistical difference at $P < 0.05$.

Figure 4. Micrographs of leaf ultrastructure of *A. donax* in control conditions with $CeCl_3$ (A) and without $CeCl_3$ (B), with excess supply of phosphorous (C, D) and without phosphorous (E, F) supply. Legend: CL: chloroplast; CW: cell wall; L: lipid body; M: mitochondrion; N: nucleus; PE: peroxisome; PL: plastoglobule; SG: starch grain; V: vacuole. Black arrows refer to electron-dense deposits of $CeCl_3$, indicative of the presence of H_2O_2. A, B, C, D: bar 1 µm; E: bar 100 nm; F: bar 2 µm.

Figure 5. Micrographs of leaf ultrastructure of *A. donax* with excess supply of sodium chloride (A, B, C), with both excess supply of phosphorous and sodium chloride (D, E, F). Legend: CL: chloroplast; CW: cell wall; L: lipid body; M: mitochondrion; N: nucleus; PE: peroxisome; PL: plastoglobule; SG: starch grain; V: vacuole. White arrows refer to wavy structure; black arrows refer to electron-dense deposits of $CeCl_3$, indicative of the presence of H_2O_2. A: bar 5 µm; B, C, D: bar 2 µm; E, F: bar 1 µm.

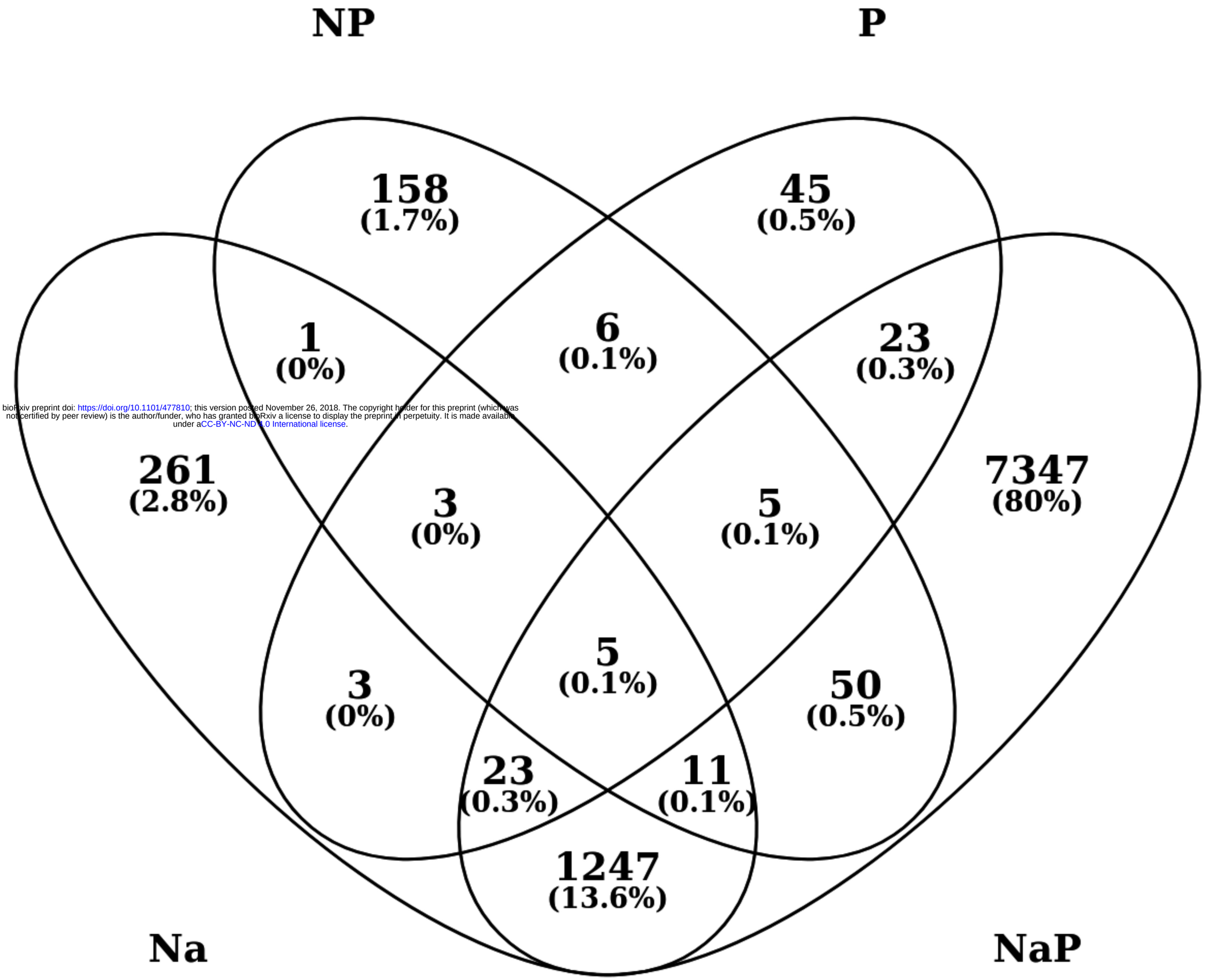

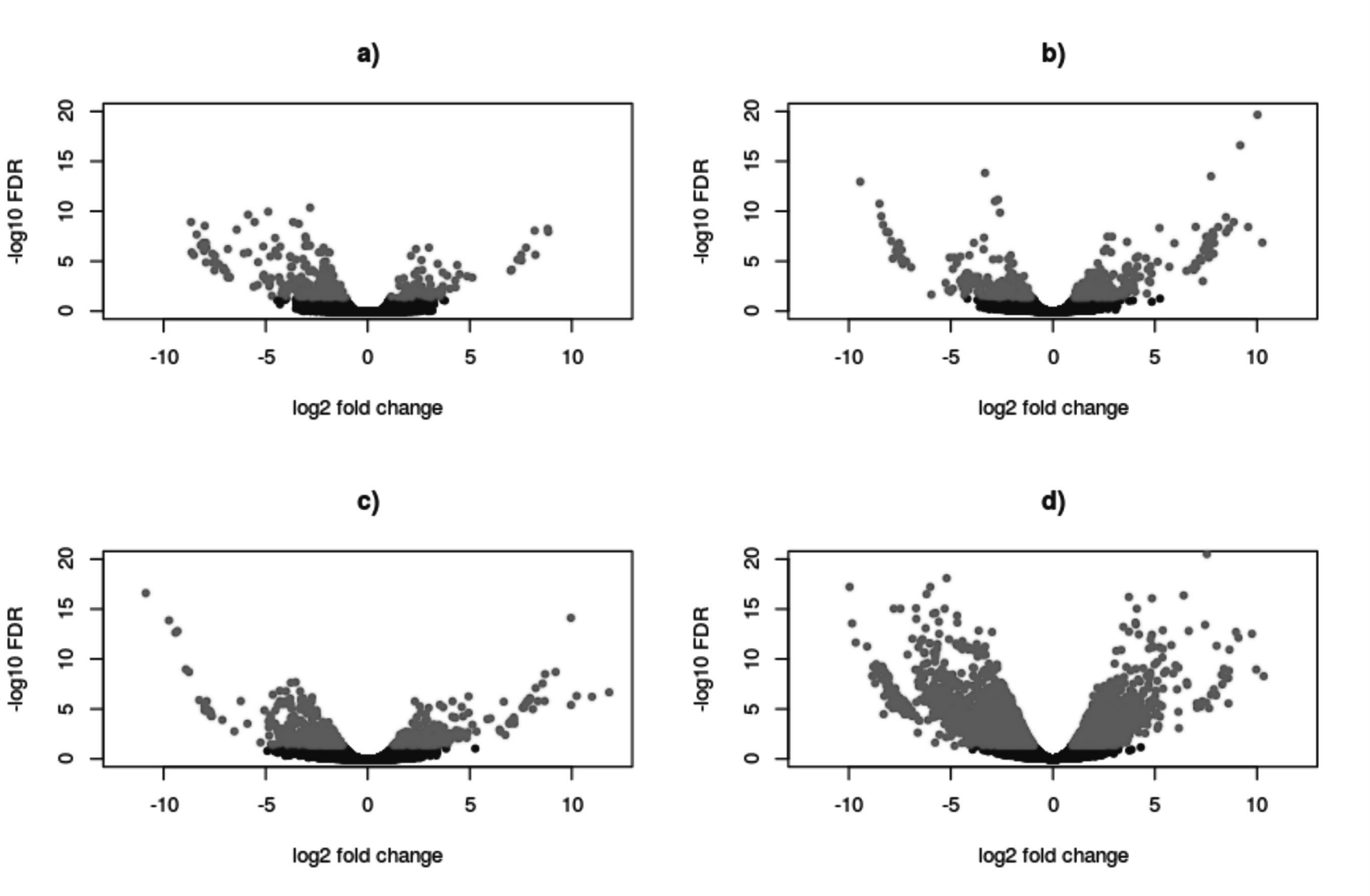
a)
b)
c)
d)
-log10 FDR
log2 fold change
0
5
10
15
20
-10
-5
0
5
10